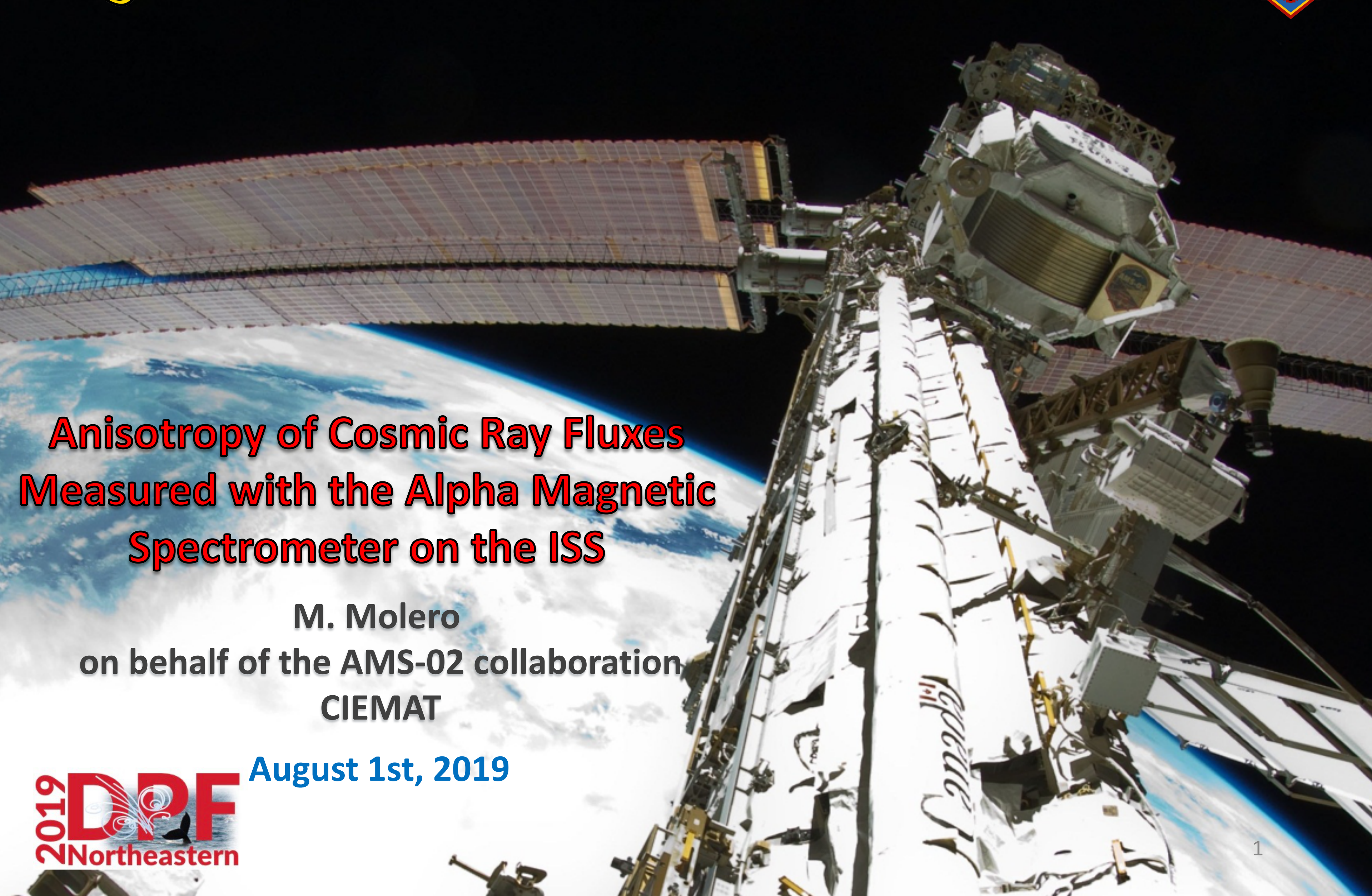

Anisotropy of Cosmic Ray Fluxes Measured with the Alpha Magnetic Spectrometer on the ISS

M. Molero
on behalf of the AMS-02 collaboration
CIEMAT

August 1st, 2019

2019 DPF Northeastern

Motivation: Protons and Light Nuclei

The proton and light nuclei fluxes cannot be described by a single power law; it shows a deviation above 200 GV

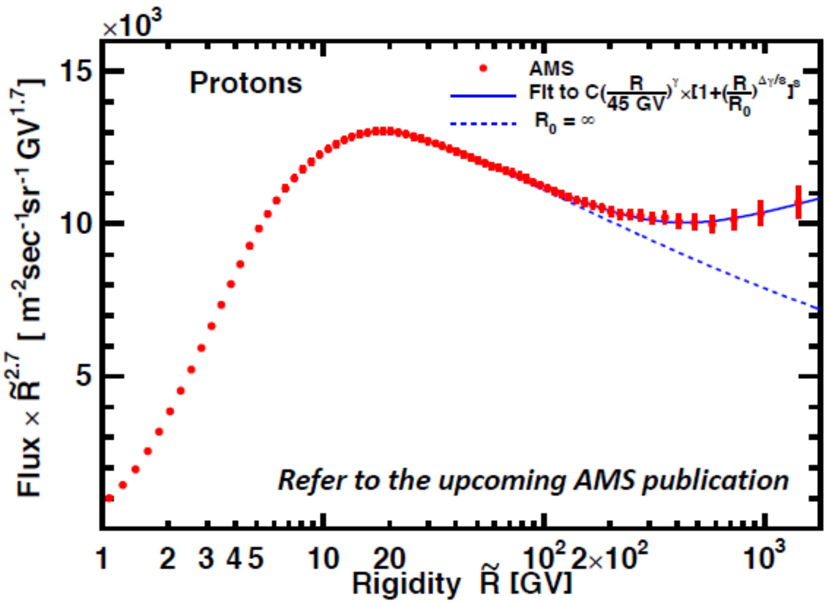

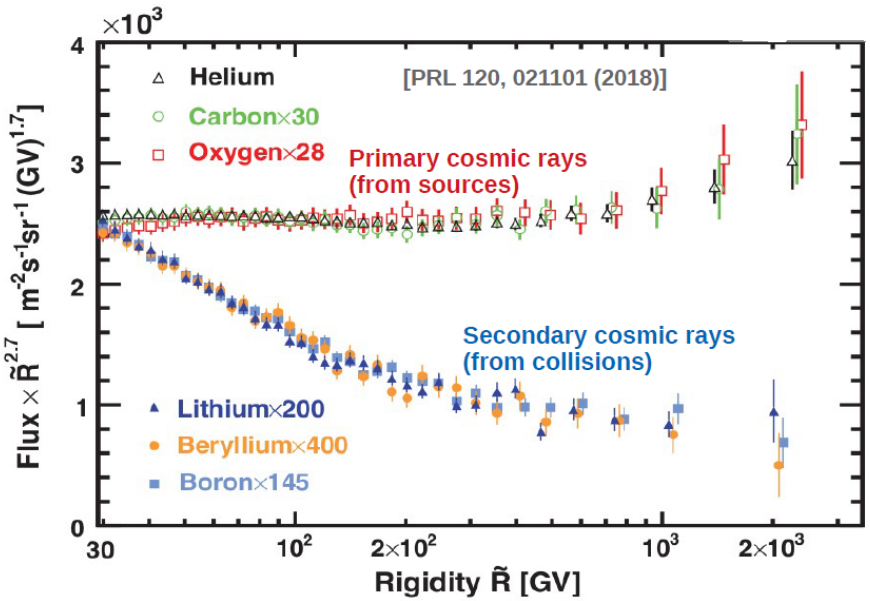

The observation may require the inclusion of local sources of high rigidity protons or nuclei a modification of CRs transport models

A nearby source of CR protons or light nuclei may induce some degree of anisotropy in the high rigidity sample

Motivation: e^+

- The positron flux shows an excess above 25 GeV that is not consistent with purely secondary production
- The excess is consistent with the existence of a source term of high-energy positrons with a characteristic cutoff energy (~800 GeV) with a significance of more than 4 sigmas

[PRL 122, 041102 (2019)]

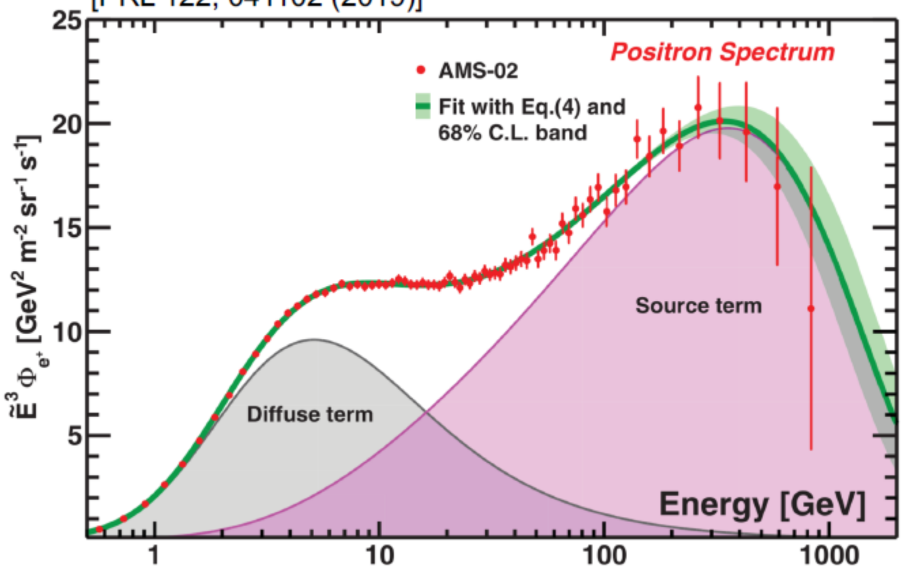

Typically the source term is classified in two scenarios: astrophysical sources and dark matter

A local source of CR positrons may induce some degree of anisotropy

Motivation: e^-

- The electron flux shows an excess above 42 GeV that is not consistent with low energy trends
- The flux does not have an energy cutoff below 1.9 TeV

[PRL 122, 101101 (2019)]

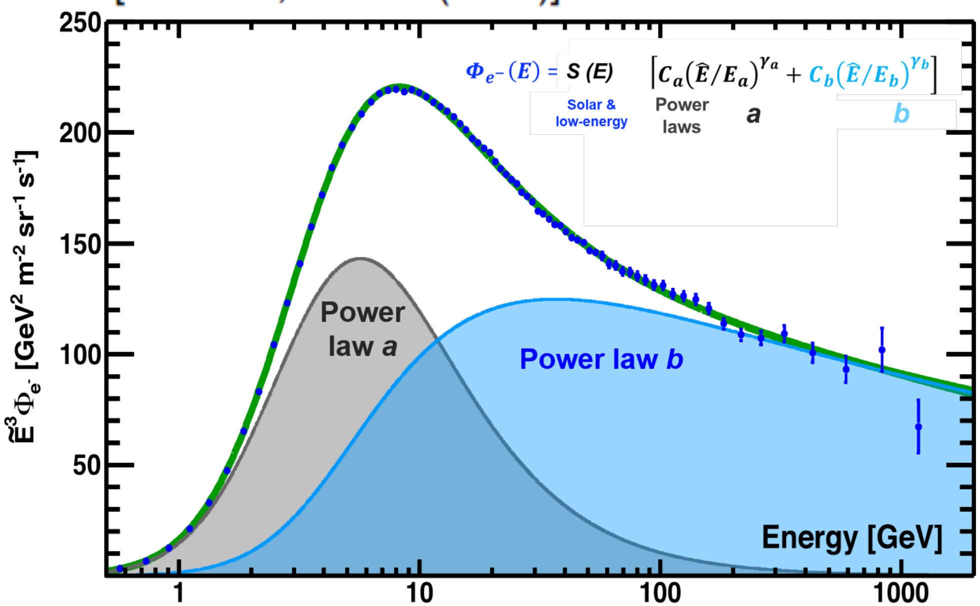

The origin of the electron excess comes from a different source than in positrons

A local source of CR electrons may induce some degree of anisotropy

Coordinate System of Analysis

Galactic Coordinates

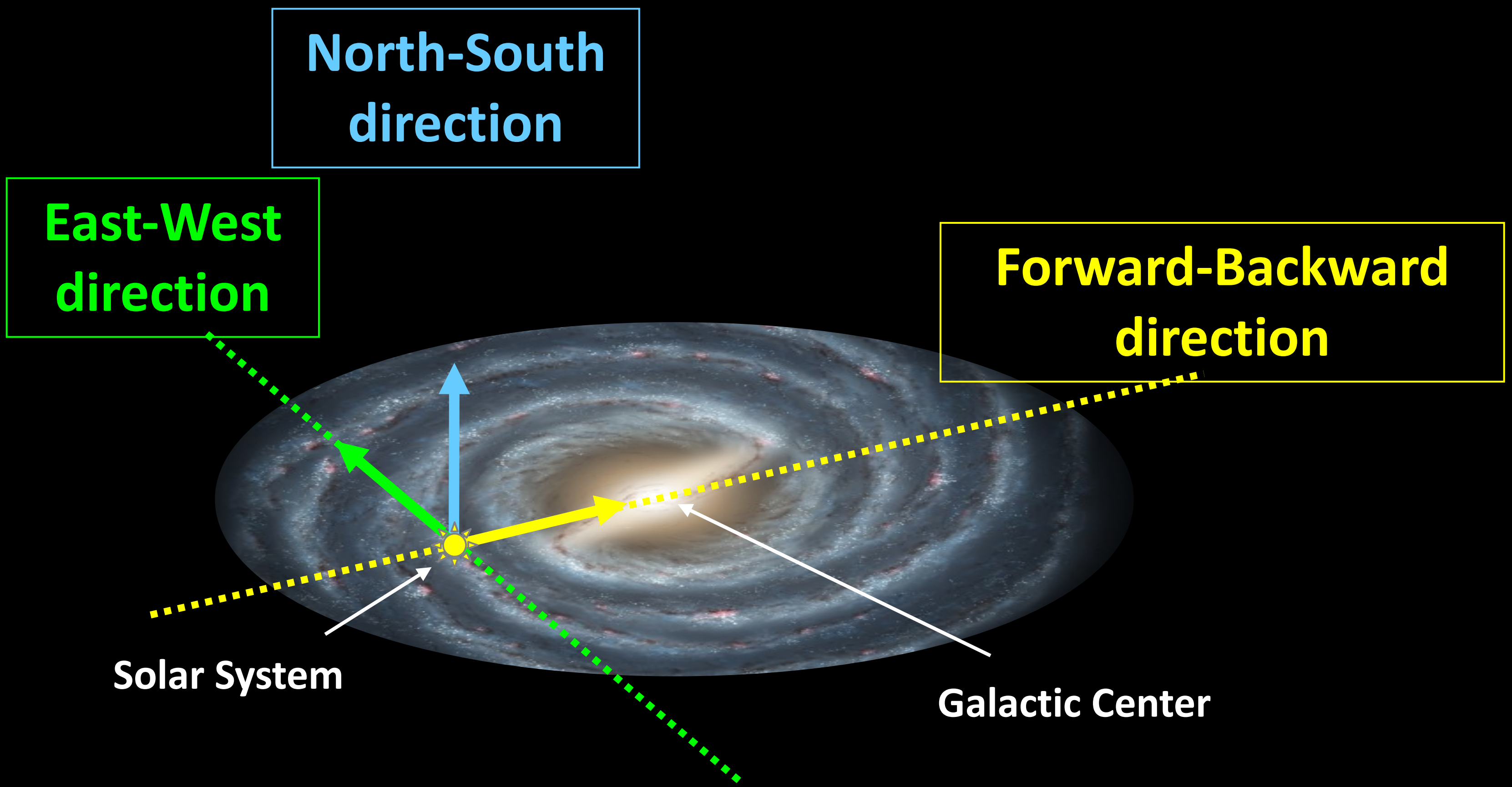

Exposure of AMS-02

Geographic Coordinates

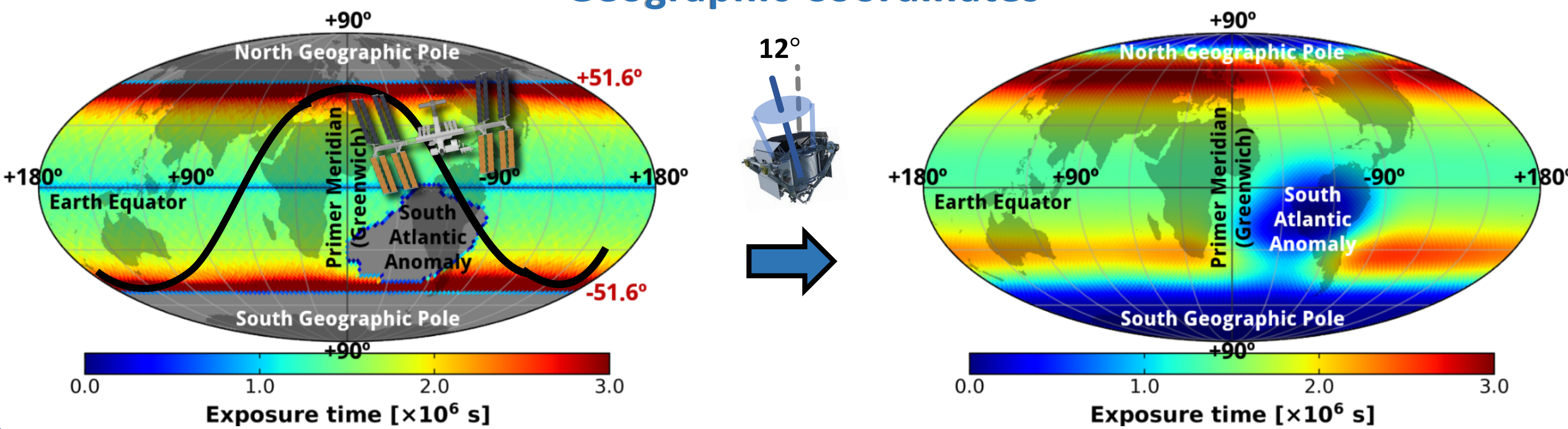

Galactic Coordinates

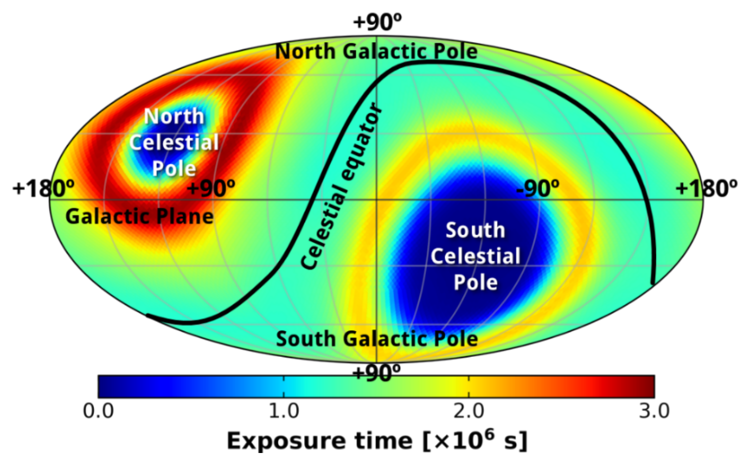

Expansion of the CRs Flux

$$\Phi(\theta,\varphi) = \Phi_0 \left(1 + \sum_{\ell=1} \sum_{m=-\ell}^{m=+\ell} a_{\ell m} Y_{\ell m}(\theta,\varphi) \right)$$

Multipolar Components

Real basis of spherical harmonics

Dipole Components

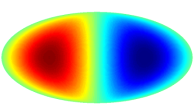

East-West $\rho_{\mathrm{EW}} = \sqrt{\frac{3}{4\pi}} a_{1-1}$

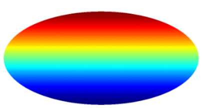

North-South $\rho_{\mathrm{NS}} = \sqrt{\frac{3}{4\pi}} a_{1+0}$

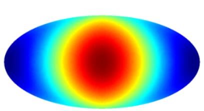

Forward-Backward $\rho_{\mathrm{FB}} = \sqrt{\frac{3}{4\pi}} a_{1+1}$

Dipole Amplitude

$$\delta = \frac{\Phi_{\max} - \Phi_{\min}}{\Phi_{\max} + \Phi_{\min}} = \sqrt{\rho_{\mathrm{EW}}^2 + \rho_{\mathrm{NS}}^2 + \rho_{\mathrm{FB}}^2}$$

Proton Anisotropy

The arrival directions of **Proton** events for the first **7.5 years** of data taking are compared to the expected map for an **isotropic** flux

# of protons ($R > 18\ GV$):
1.3×10^{8}

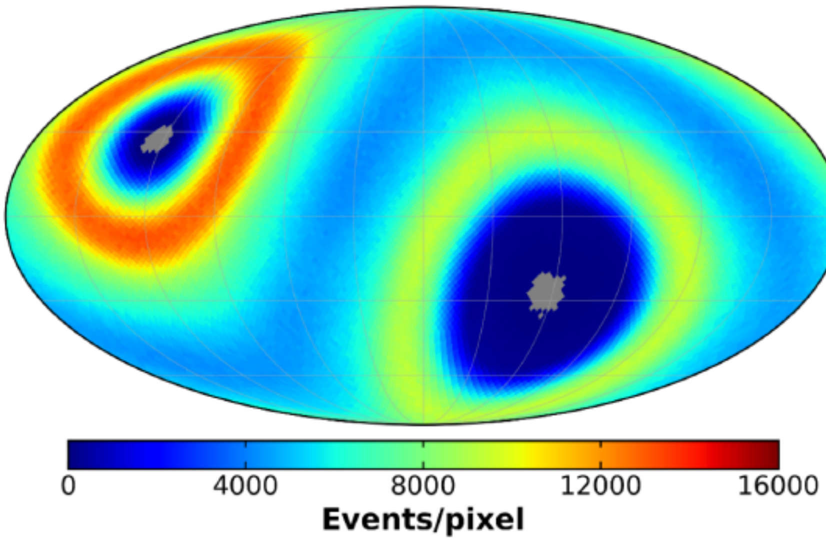

Isotropic Map

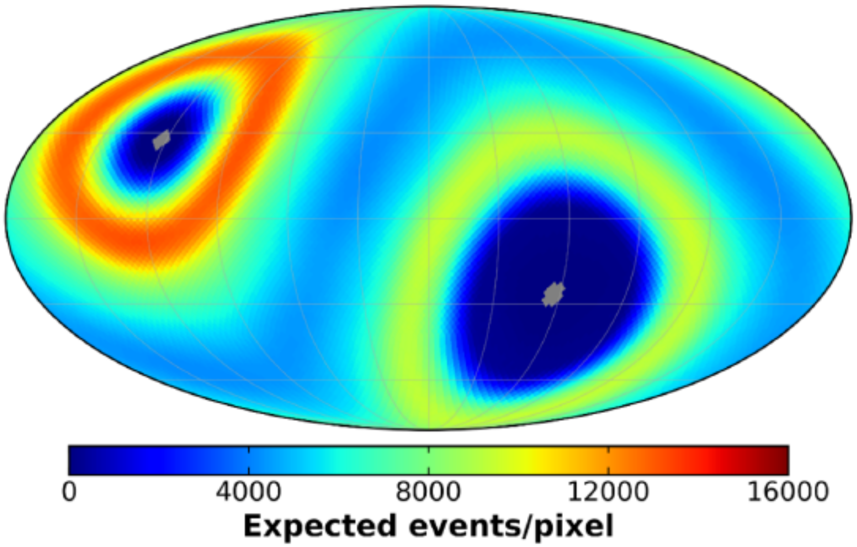

Selected events are grouped into 9 cumulative rigidity ranges:

R > 18, 30, 45, 80, 150, 200, 300, 500, 1000 GV

Proton Detector Efficiencies

Computation of isotropic map requires detailed understanding of **detector efficiencies** at different geographical locations

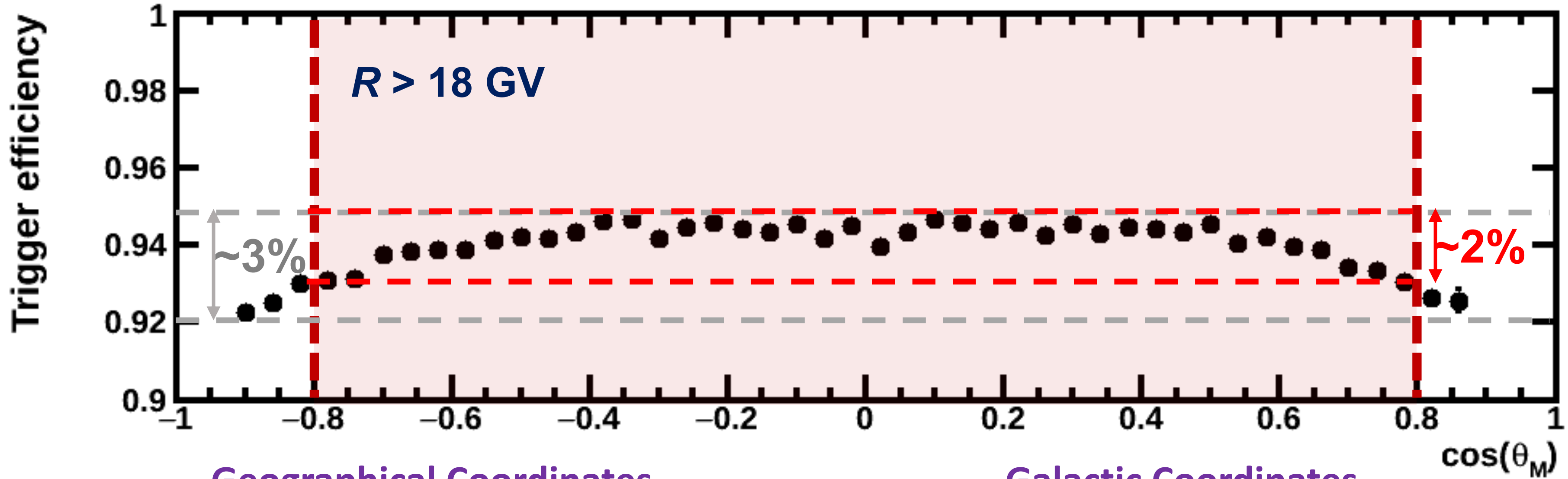

Geographical Coordinates

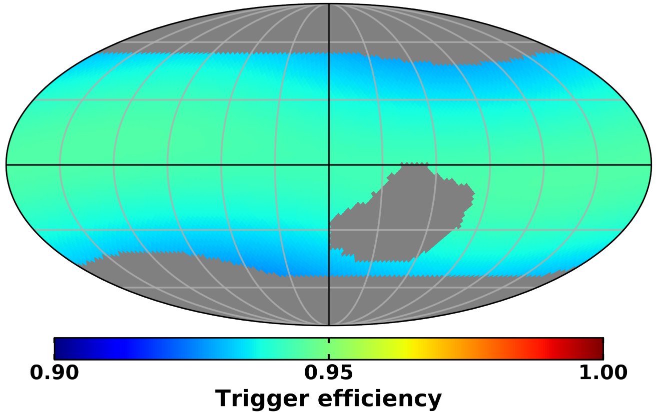

Galactic Coordinates

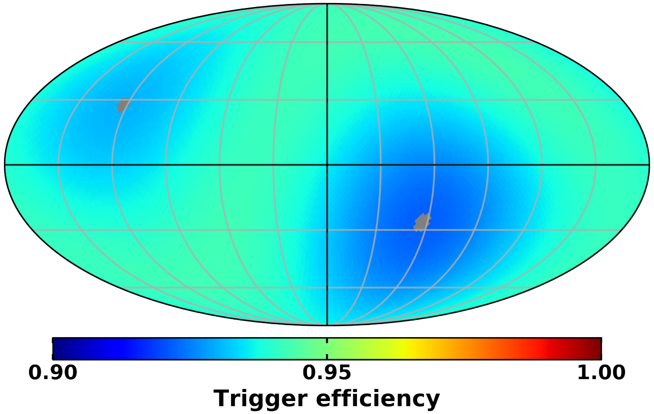

Proton Detector Efficiencies

Corrections on individual components are computed for each selection efficiency to produce the corrected isotropic map

Galactic Coordinates

Individual efficiency corrections

Total efficiency correction

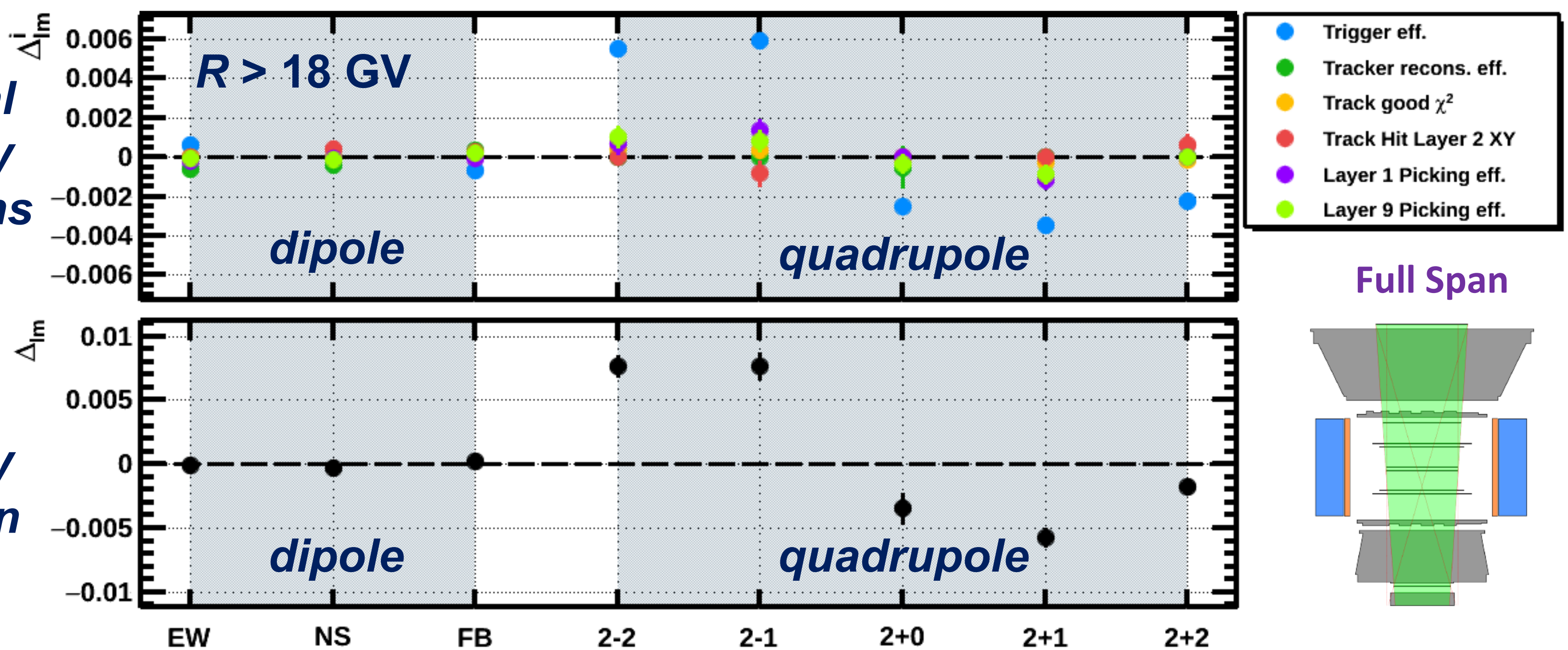

Proton Anisotropy: Dipole Components

Galactic Coordinates

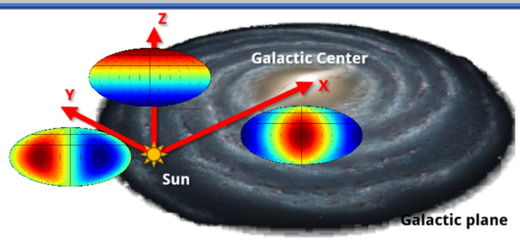

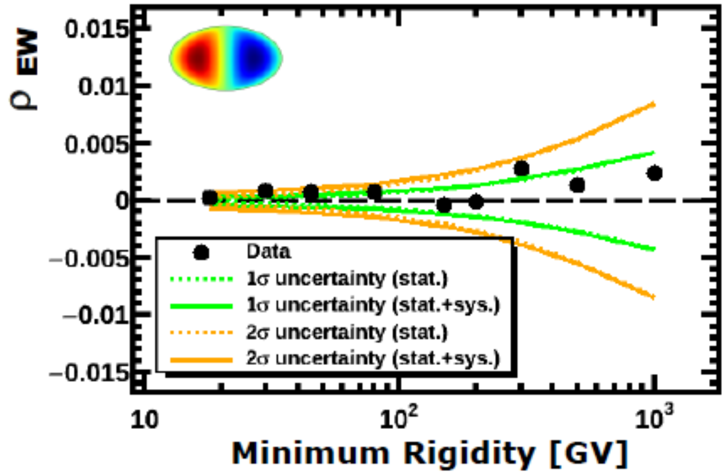

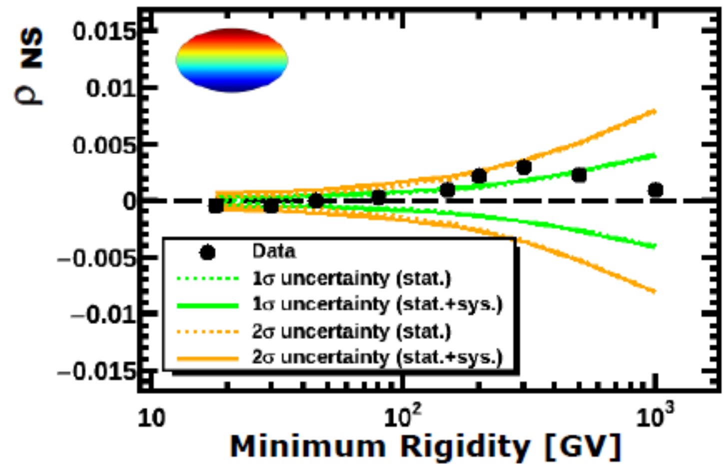

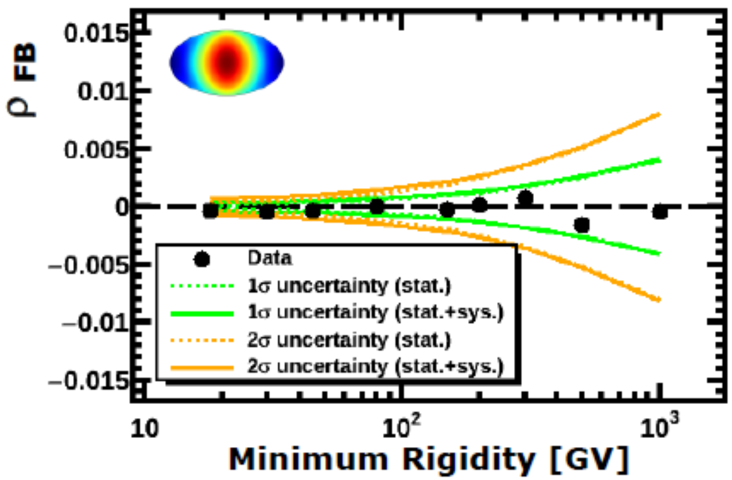

Dipole components are consistent with isotropy

Proton Anisotropy: δ Upper Limit

Proton data is consistent with isotropy for all rigidity ranges

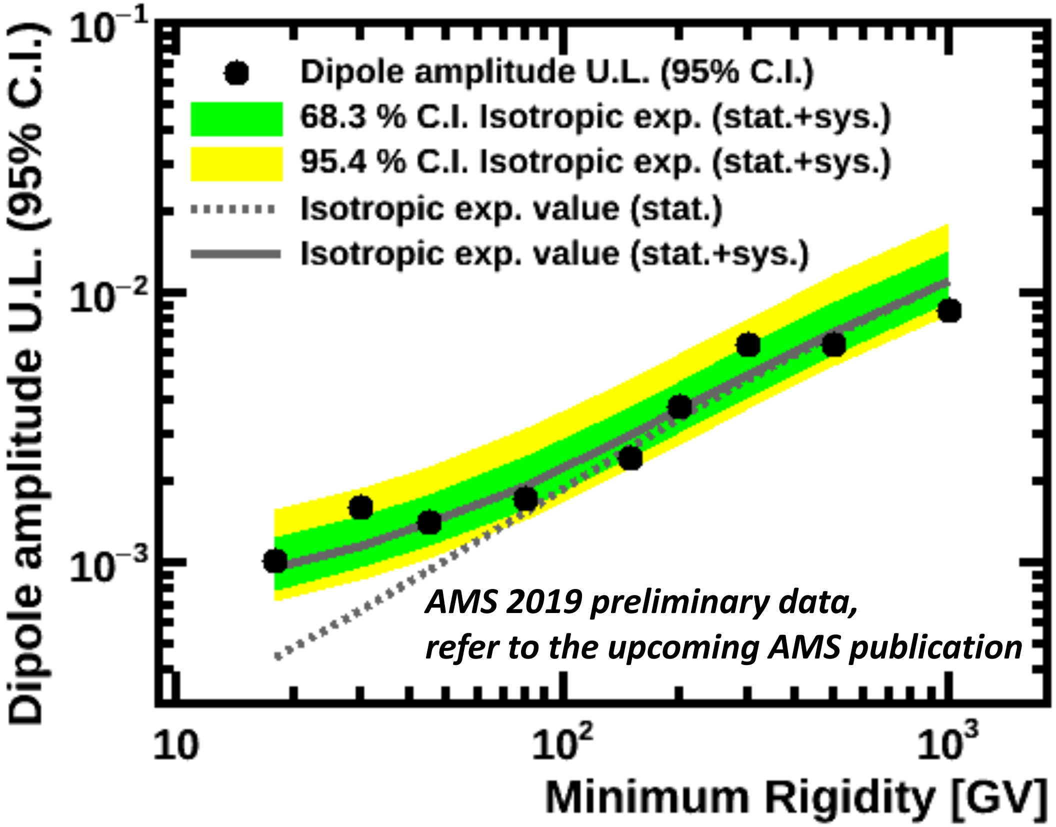

δ (R > 200 GV) < 0.38% at 95% C.I.

Helium Anisotropy

The arrival directions of Helium events for the first 7.5 years of data taking are compared to the expected map for an isotropic flux

# of Helium ($R > 18\ GV$): 1.0×10^8

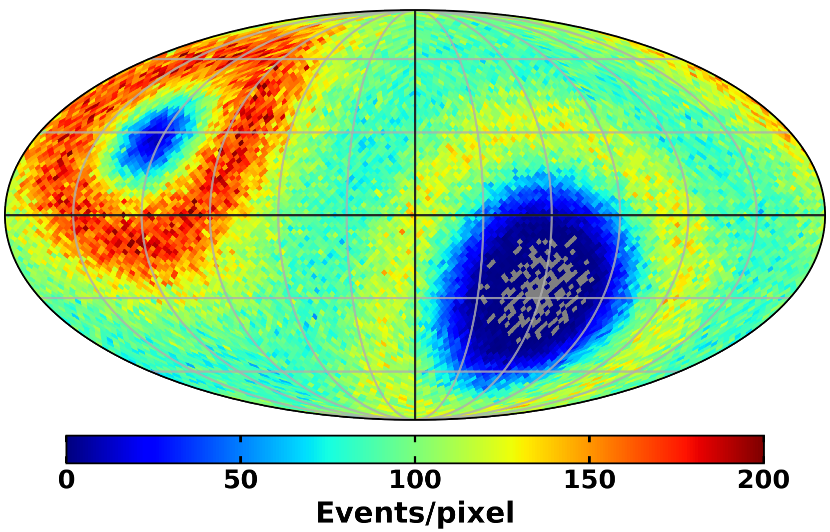

Isotropic Map

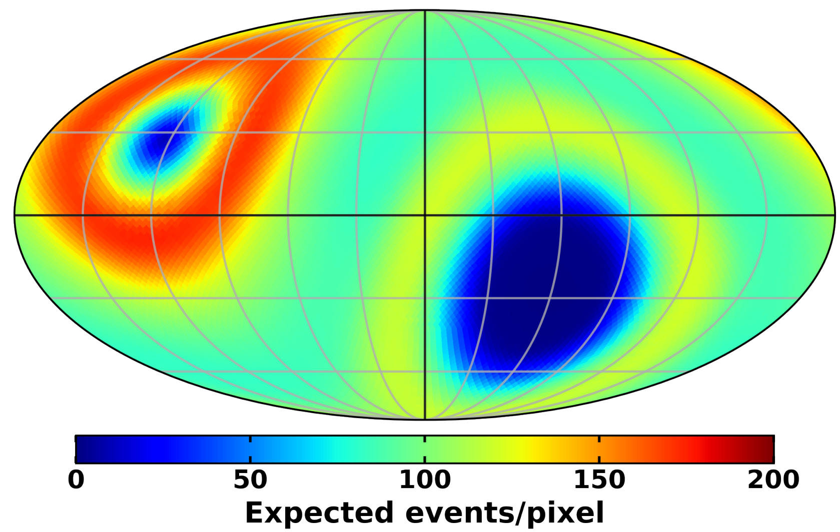

Helium Detector Efficiencies

Reduced amplitude of the geographical dependence of the detector efficiencies allows to use extended detector acceptance

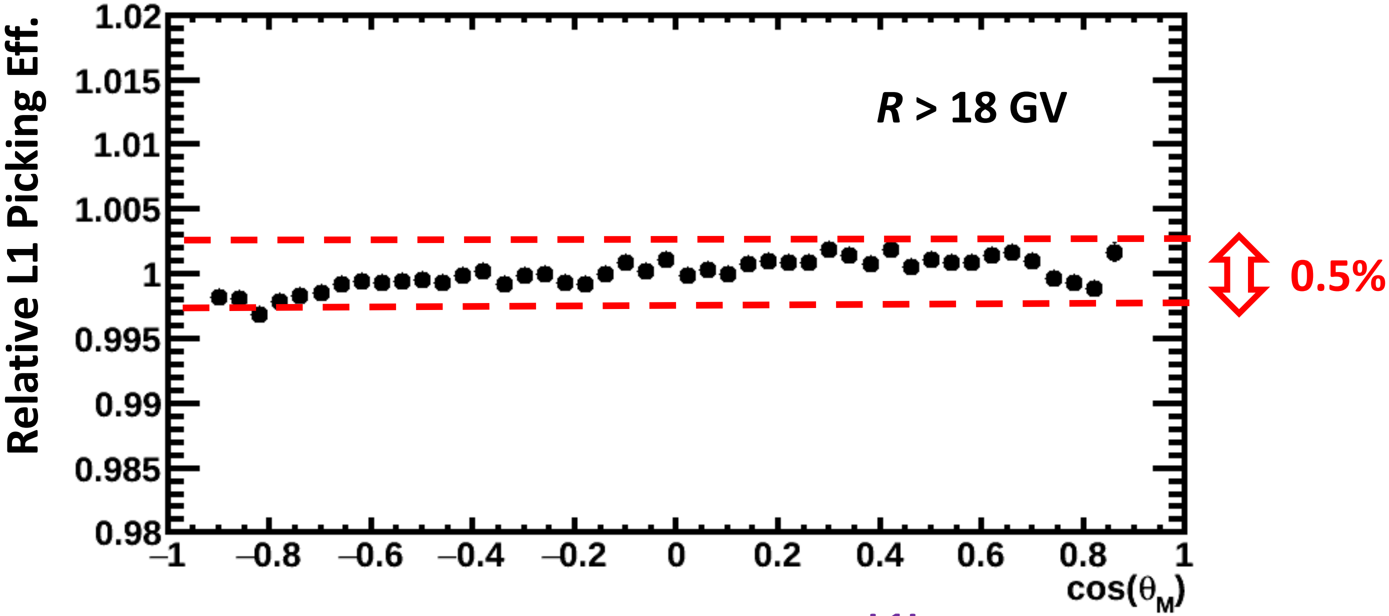

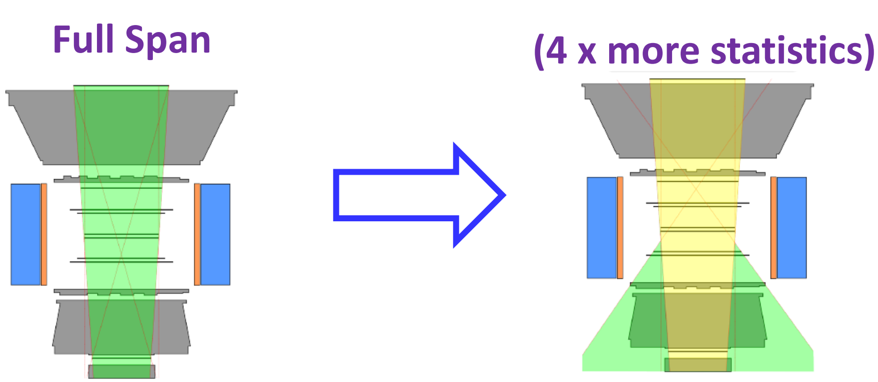

Helium Anisotropy: δ Upper Limit

Helium data is consistent with isotropy for all rigidity ranges

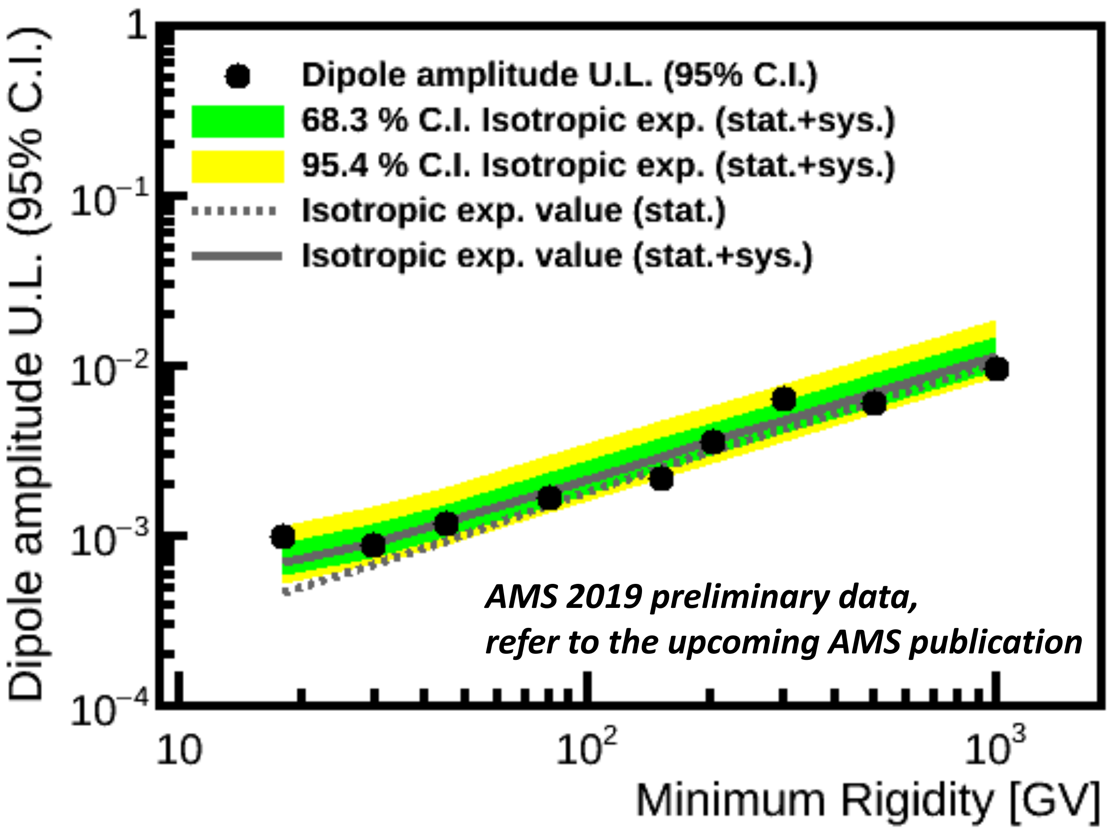

δ (R > 200 GV) < 0.36% at 95% C.I.

Carbon and Oxygen Anisotropy: δ Upper Limit

- Same analysis as in Helium is applied for Carbon and Oxygen
- Carbon and Oxygen data are consistent with isotropy for all rigidity ranges

# of Carbon ($R > 200\ GV$): 6.1×10^4

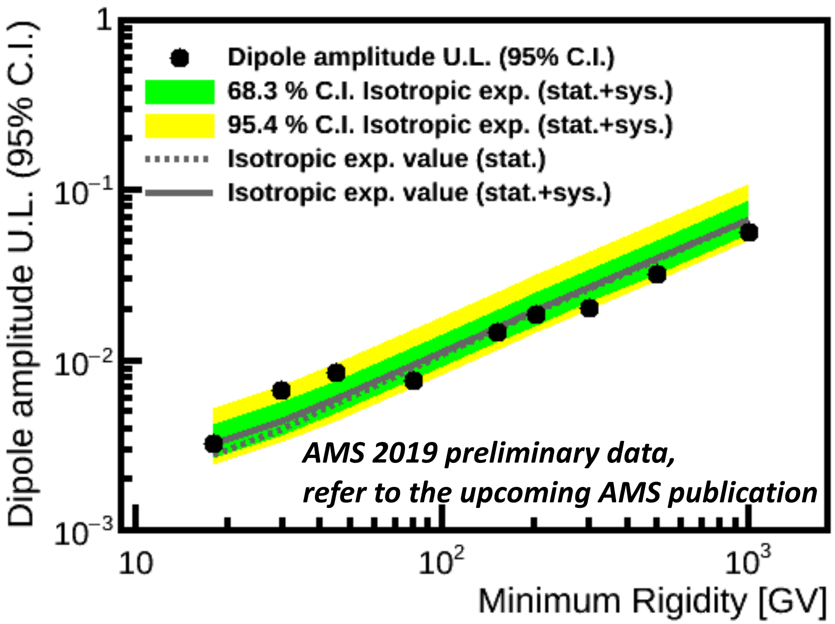

δ (R > 200 GV) < 1.9% at 95% C.I.

# of Oxygen ($R > 200\ GV$): 6.3×10^4

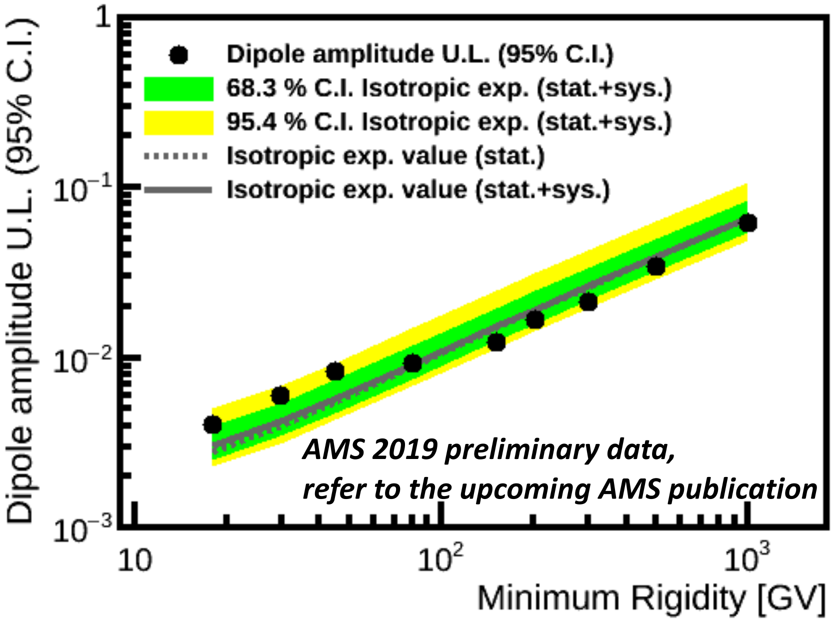

δ (R > 200 GV) < 1.7% at 95% C.I.

Positron and Electron Anisotropy

The arrival directions of Positron and Electron events for the first 6.5 years of data taking are compared to the expected map for an isotropic flux

# of e^{+} $(16-350\ GeV)$: 9.9×10^{4}

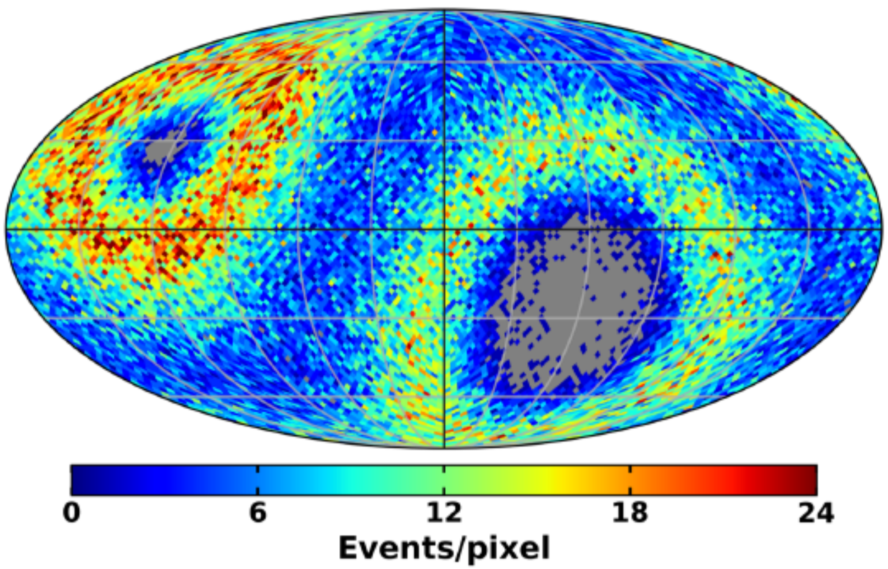

# of e^{-} $(16-350\ GeV)$: 1.3×10^{6}

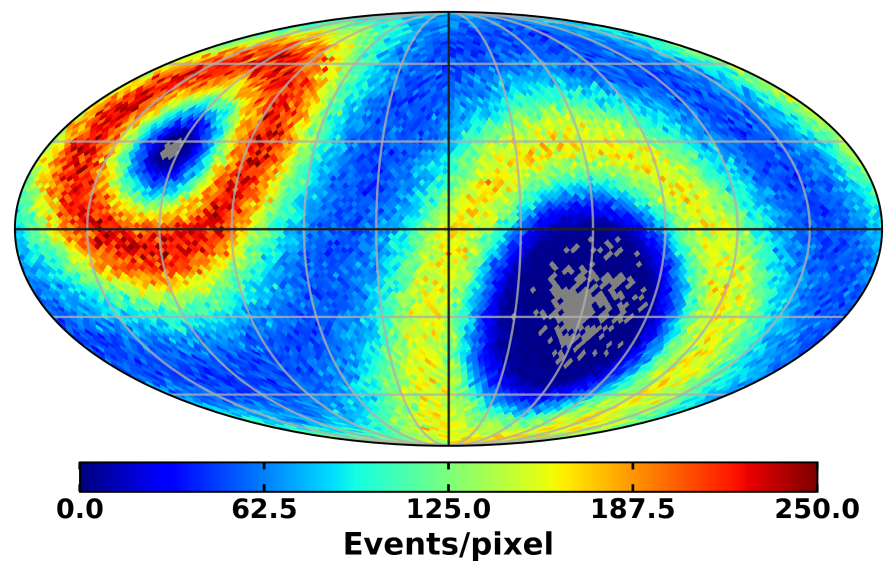

Selected events are grouped into 5 cumulative energy ranges:

E > 16, 25, 40, 65, 100 GeV

Positron and Electron Anisotropy: δ Upper Limit

The positron and electron data are consistent with isotropy and limits to the dipole amplitude are set

Positron

[PRL 122, 041102 (2019)]

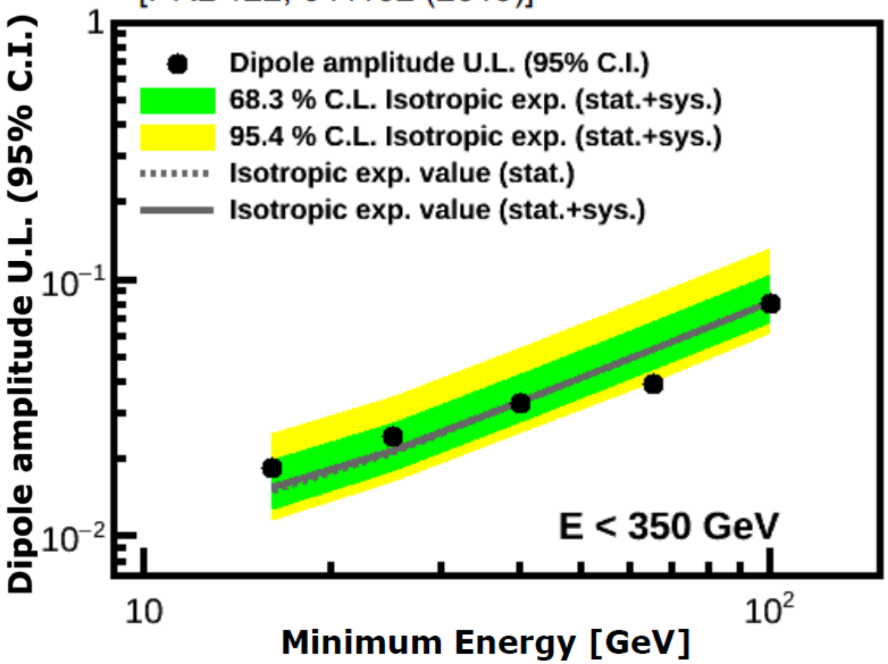

δ (16-350 GeV) < 1.9% at 95% C.I.

Electron

[PRL 122, 101101 (2019)]

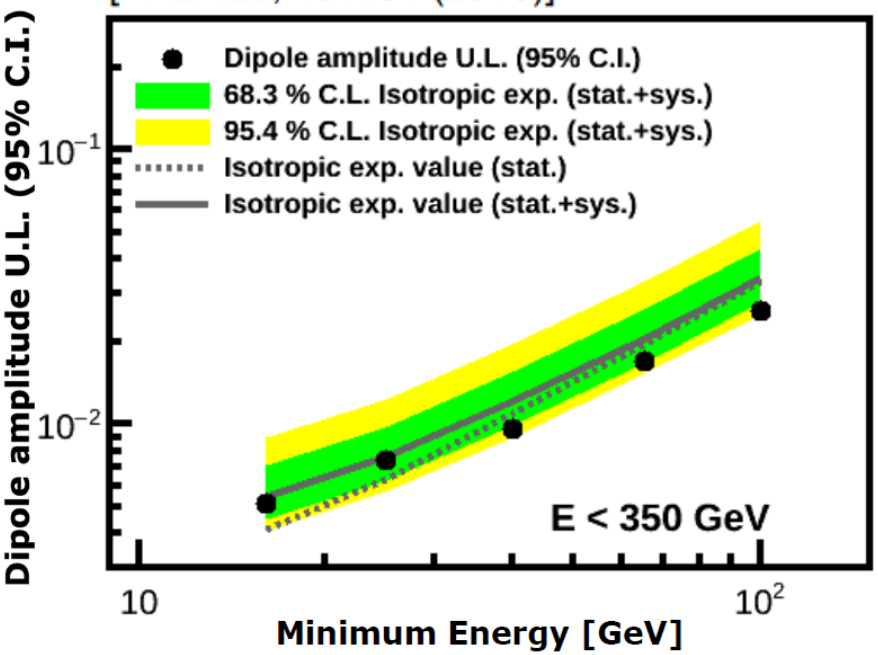

δ (16-350 GeV) < 0.5% at 95% C.I.

Conclusions

- AMS measurements show new features in the positron, electron, proton and light nuclei fluxes which challenge the traditional propagation models
- The study of the anisotropy allows us to understand its origin
- Proton, Helium, Carbon and Oxygen are consistent with isotropy for $R >$ 200 GV and upper limits to the dipole amplitude (95% C.I) can be set as:
  - Proton: δ < 0.38 %
  - Helium: δ < 0.36 %
  - Carbon: δ < 1.90 %
  - Oxygen: δ < 1.70 %
- Positrons and electrons in the energy range of 16-350 GeV are also consistent with isotropy and upper limits to the dipole amplitude (95% C.I) δ < 1.9 % and δ < 0.5 % are obtained, respectively
- AMS will continue taking data until the end of ISS operation, currently 2024. By that time positron statistics will allow us to reach the 1% level predicted by pulsars models